International Journal of Remote Sensing
Vol. 28, No. 19, 10 October 2007, 4311–4330

Taylor & Francis
Taylor & Francis Group

A ground-validated NDVI dataset for monitoring vegetation dynamics and mapping phenology in Fennoscandia and the Kola peninsula

P. S. A. BECK*†, P. JÖNSSON‡, K.-A. HØGDA§,
S. R. KARLSEN§, L. EKLUNDH¶ and
A. K. SKIDMORE‖

†Department of Biology, University of Tromsø, N-9037 Tromsø, Norway
‡Teachers Education, Malmö University, SE-205 06 Malmö, Sweden
§NORUT IT AS, N-9291 Tromsø, Norway
¶Department of Physical Geography and Ecosystems Analysis, Lund University, Sölvegatan 12, SE-223 62 Lund, Sweden
‖International Institute for Geo-Information Science and Earth Observation (ITC), PO Box 6, 7500 AA Enschede, The Netherlands

(*Received 17 August 2006; in final form 24 November 2006*)

An NDVI dataset covering Fennoscandia and the Kola peninsula was created for vegetation and climate studies, using Moderate Resolution Imaging Spectroradiometer 16-day maximum value composite data from 2000 to 2005. To create the dataset, (1) the influence of the polar night and snow on the NDVI values was removed by replacing NDVI values in winter with a pixel-specific NDVI value representing the NDVI outside the growing season when the pixel is free of snow; and (2) yearly NDVI time series were modelled for each pixel using a double logistic function defined by six parameters. Estimates of the onset of spring and the end of autumn were then mapped using the modelled dataset and compared with ground observations of the onset of leafing and the end of leaf fall in birch, respectively. Missing and poor-quality data prevented estimates from being produced for all pixels in the study area. Applying a 5 km × 5 km mean filter increased the number of modelled pixels without decreasing the accuracy of the predictions. The comparison shows good agreement between the modelled and observed dates (root mean square error=12 days, n=108 for spring; root mean square error=10 days, n=26, for autumn). Fennoscandia shows a range in the onset of spring of more than 2 months within a single year and locally the onset of spring varies with up to one month between years. The end of autumn varies by one and a half months across the region. While continued validation with ground data is needed, this new dataset facilitates the detailed monitoring of vegetation activity in Fennoscandia and the Kola peninsula.

1. Introduction

Time series of vegetation indices based on satellite observations were first created in the 1980s and have continuously grown in importance for ecological and other biosphere-related research (Justice *et al.* 1985, Malingreau 1986, Pettorelli *et al.* 2005a). As vegetation indices reflect vegetation characteristics connected with the chemical components in leaves and the structure and density of the canopy, they are

*Corresponding author. Email: pieter.beck@ib.uit.no

International Journal of Remote Sensing
ISSN 0143-1161 print/ISSN 1366-5901 online © 2007 Taylor & Francis
http://www.tandf.co.uk/journals
DOI: 10.1080/01431160701241936

used, for example, for mapping vegetation (Azzali and Menenti 2000) and biodiversity (Oindo and Skidmore 2002), and for estimating the leaf area index (Baret and Guyot 1991). Vegetation indices are also of great value for understanding the temporal dynamics of productivity and the phenology of terrestrial ecosystems (Schwartz *et al*. 2002, White *et al*. 2002). Understanding changes in phenology is important, as alterations in the timing of phenological events are among the first responses at plant and ecosystem levels to climate change (Badeck *et al*. 2004).

Temporal analysis of vegetation indices ranges from the comparison of two images (e.g. Malingreau and Tucker 1988) to the analysis of data series spanning 10 years or more (e.g. Zhou *et al*. 2001, Anyamba and Tucker 2005). Often, the time series are used for mapping vegetation phenology (Gong and Shi 2003, Suzuki *et al*. 2003, Walker *et al*. 2003, de Beurs and Henebry 2005). These maps provide a means of investigating the effects that present and future climatic variations have and will have on vegetation (Wang *et al*. 2003, Zhang *et al*. 2003a, b, Zhou *et al*. 2003), as well as potential feedback effects of vegetation on climate (Wylie *et al*. 2003, Picard *et al*. 2005). In climate studies, vegetation index time series have proven useful for modelling CO_2 fluxes (Goetz and Prince 1996, Walker *et al*. 2003). In addition, net primary productivity and plant biomass have been successfully modelled using time-integrated NDVI (Høgda and Tømmervik 1998). In terrestrial ecology, the vegetation index time series have very wide applications for studies at landscape scale, for example, for the mapping of insect plagues (Duchemin 1999) and water stress (Oindo and Skidmore 2002, Bailey *et al*. 2004), and the prediction of plant and animal species richness (Pettorelli *et al*. 2005b) or the body mass of reindeer calves (Delbart *et al*. 2005).

The Normalized Difference Vegetation Index (NDVI) is the most commonly used vegetation index. It quantifies the contrast between red surface reflectance (ρ_{RED}), which decreases with increasing chlorophyll content, and near-infrared surface reflectance (ρ_{NIR}), which increases with growing leaf area index and crown coverage:

$$\mathrm{NDVI} = (\rho_{\mathrm{NIR}} - \rho_{\mathrm{RED}})/(\rho_{\mathrm{NIR}} + \rho_{\mathrm{RED}}). \quad (1)$$

Atmospheric noise in the NDVI caused by clouds, dust and aerosols is generally considered negatively biased. This is because additive path radiance causes an increase in red reflectance, while lower atmospheric transmission reduces near-infrared reflectance (Guyot *et al*. 1989). Maximum value compositing (MVC, Holben 1986) is a common method of eliminating noise from NDVI series, as well as errors due to sensor-related artefacts such as line dropout. In this method, only the highest NDVI value in a predefined compositing period is retained. This results in fewer but more reliable NDVI values representing the time series.

MVC NDVI datasets have been created using data from sensors with large swath widths and aboard satellites with short revisit periods, for example, the National Oceanic and Atmospheric Administration (NOAA) Advanced Very High Resolution Radiometer (AVHRR) and the VEGETATION (VGT) sensor aboard Satellite Probatoire d'Observation de la Terre (SPOT). Inception dates of these datasets are 1981 and 1998, respectively, and the MVC products are available at spatial resolutions starting at about 1 km. Since 2000, MVC products have been available from the Moderate Resolution Imaging Spectroradiometer (MODIS) aboard the TERRA and AQUA satellites. Compared with the NOAA-AVHRR, MODIS features improved calibration and atmospheric correction, and the MVC

NDVI is produced at a spatial resolution of 250 m and compositing intervals of 16 days.

Often, NDVI time series resulting from MVC contain abrupt temporal changes in NDVI values. These are considered as errors when they are inconsistent with the relatively gradual manner in which vegetation activity changes in time. The changes are due mostly to persistent cloud cover and bidirectional reflectance distribution function (BRDF) effects (Los *et al*. 2005). Smoothing and modelling techniques are used to eliminate such errors, often relying on fitting functions to the time series and replacing the MVC values with the values predicted by the functions (e.g. Jönsson and Eklundh 2002, Chen *et al*. 2004). The negative bias in the errors is accounted for by giving high NDVI values a greater weight in the fitting algorithm used to estimate the parameters of the functions.

NOAA-AVHRR MVC products have been used to create smoothed datasets at global (Los *et al*. 1994, Sellers *et al*. 1994) and regional scales (Stöckli and Vidale 2004, Heumann *et al*. 2007). The low spatial resolution of these datasets, with pixel sizes of a square kilometre or more, makes it difficult to validate derived phenological maps with *in situ* observations of vegetation phenology, which generally refer to just a few or even single plants. With MVC datasets of higher spatial resolution, however, it should become possible to monitor vegetation dynamics in greater detail from space and, more importantly, to validate the results obtained from vegetation index time series with phenological ground observations. The spatial resolution of the MODIS MVC products should also facilitate ecological research into more local processes, and at larger scales than hitherto possible.

Fennoscandia comprises Norway, Sweden, and Finland, and it harbours the most northern forest ecosystems in Europe. The region displays very steep and broad climatic gradients from north to south, from oceanic to continental, and from lowland to alpine (Tuhkanen 1980, Moen 1999). As global warming is expected to be particularly pronounced at northern latitudes (McCarthy *et al*. 2001), and the region is bioclimatically diverse, monitoring changes in vegetation activity across Fennoscandia is important. So far, this has been done using the GIMMS dataset, which is a 15-day MVC dataset with an 8-km spatial resolution and based on data from the NOAA-AVHRR sensors (Høgda and Tømmervik 1998, Høgda *et al*. 2001, 2002). This resolution limits the degree to which the remote-sensing data can be related to ground-based vegetation phenology measurements and to which they can be used for local studies.

Here, we present a smoothed NDVI dataset designed for monitoring vegetation activity and mapping vegetation phenology in Fennoscandia and the Kola peninsula derived from the MODIS 16-day MVC NDVI product. To illustrate the use of the dataset, we mapped the onset of spring and the end of autumn in Fennoscandia and the Kola peninsula from 2000 to 2005. The maps were validated using *in situ* observations of spring and autumn phenology in birch (*Betula* sp.), the dominant deciduous tree genus in most of the region (Bohn *et al*. 2000, Köble and Seufert 2001).

2. Methods

2.1 *Input data*

We used the 16-day composite MODIS NDVI dataset with a ground resolution of 250 m (500 m in the northernmost area), spanning the period from 2000 to 2005 (the

MOD13Q1 product, Huete *et al.* 2002). It is produced from surface reflectance data corrected for molecular scattering, ozone absorption and aerosols (Vermote *et al.* 2002). Before the compositing of the NDVI data, a filter selects cloud-free near-nadir observations. Vegetation indices usually increase when they are measured more obliquely. To buffer this effect, the compositing algorithm used for the MODIS vegetation index constrains the variation in viewing angle in the data. It compares the two highest NDVI values after filtering and selects the observation closest to nadir view to represent the 16-day composite cycle. The MVC dataset contains 23 NDVI observations per pixel per year. These observations are accompanied by auxiliary information on different parameters, such as aerosol quantity and the likelihood of snow cover, as well as an overall indication of the usefulness of each data point (scaled from 15 to 0, with 0 indicating 'perfect quality'). Data points with a usefulness index higher than 14 were deleted from the dataset. The northern data granules of two horizontal MODIS tiles (h18 and h19) were merged to cover Fennoscandia and the Kola peninsula in its entirety, and water bodies and glaciers were masked.

2.2 *Winter NDVI calculation*

The presence of snow and the polar night during winter complicates the use of NDVI time series for modelling vegetation activity at high latitudes. As snow has a negative effect on the NDVI, the disappearance of snow at the end of winter causes the NDVI to rise. However, this rise does not necessarily coincide with increased vegetation activity. Hence, the NDVI of a pixel outside the growing season (which we term 'winter NDVI') needs to be estimated (Beck *et al.* 2006).

In spring, there are often only a few days between the disappearance of snow and the onset of greenness—or these events may even overlap—and ideally the winter NDVI is observed after the growing season and before the arrival of snow. However, in the MODIS NDVI MVC dataset, the observations after the growing season are in most areas of poor quality, as indicated by the usefulness index. Hence, we used NDVI data collected prior to the growing season (February–March) and combined them with NDVI data collected after the growing season (October–November) to estimate the winter NDVI. This was done by initially estimating the winter NDVI based solely on the February–March data. For each of the two horizontal tiles, we selected the NDVI scenes between 18 February and 21 March of the highest quality (table 1). For each pixel, we used the usefulness index to extract

Table 1. Acquisition dates of the MODIS NDVI images used for the first approximation of the NDVI of a pixel outside the growing season (winter NDVI).

	18 February–5 March	6–21 March
2000		X
2001	X	X
2002		X
2003		X
2004		h18
2005	X	X

The study area is covered by MODIS tiles h18 and h19. X indicates that images of both tiles were used for a given date; h18 indicates that images of tile h18 only were used.

the most reliable values in the available images, after excluding very high NDVI values (NDVI >0.95) and values with a usefulness index worse than 12. We then calculated an initial estimate of the winter NDVI for a pixel as the median of the five values of highest quality based on the usefulness index. If fewer than five values were extracted for a pixel, the median of all extracted values was used. By using the ancillary data on snow, we noted for each pixel whether the median value was likely to be influenced by snow, so it could be adjusted later on.

The initial estimates of the winter NDVI derived from the NDVI data of February and March were probably negatively biased if snow was present. To correct for this bias, we considered the relationship between the initial winter NDVI estimates derived from the February and March data (wNDVI*) and the winter NDVI estimates derived from the October and November data for an area with high-quality data after the growing season (wNDVI, Beck *et al*. 2006). When it was higher than 0.3, the wNDVI correlated with the wNDVI* (figure 1). The relationship can be described by an asymptotic exponential with intercept 0.3 (root mean square error (RMSE)=0.12; figure 1):

$$\mathrm{wNDVI} = 0.3 + 0.5 \times (1 - \exp(-5.7(\mathrm{wNDVI}))). \quad (2)$$

As it was possible that the wNDVI estimates contained a small negative bias (Beck *et al*. 2006), the curve was first fitted using a least-squares procedure and was then adjusted upwards manually so that higher rather than lower wNDVI values were estimated.

The exponential function (equation (2)) was used to adjust those initial winter NDVI estimates that, as registered in the initial calculation, were affected by snow. As a result of the intercept of the function, all winter NDVI values lower than 0.3 were set to 0.3. This value is comparable to thresholds set by other authors defining NDVI values below which changes in NDVI are not related to major changes in vegetation dynamics. Suzuki *et al*. (2003) chose 0.2 using an AVHRR-NDVI dataset, and Delbart *et al*. (2005) chose 0.4 with SPOT-VGT.

For each pixel and year, the NDVI values during the winter period from 17 November to 21 March were replaced with the winter NDVI value for that pixel.

2.3 *Double logistic curve as a smoothing and interpolation tool*

Boreal, alpine, and arctic vegetation is characterized by a short growing season, with a rapid transition from vegetation dormancy to activity. Each year, this results in a unimodal NDVI trajectory that can show a sudden rise in NDVI during spring and a short period with higher NDVI values in summer. Beck *et al*. (2006) showed that a double logistic function is suitable for modelling such trajectories observed in a single year in boreal and arctic–alpine vegetation. The double logistic function models the NDVI as a function of time (t), using six parameters. These are the minimum and maximum NDVI (wNDVI and mNDVI), two inflection points (S and A), and parameters related to the rate of increase or decrease in NDVI at S and A, respectively (mS and mA, figure 2):

$$\mathrm{NDVI}(t) = \mathrm{wNDVI} + (\mathrm{mNDVI} - \mathrm{wNDVI}) \times \left(\frac{1}{1 + \exp(-mS \times (t - S))} + \frac{1}{1 + \exp(mA \times (t - A))} - 1 \right). \quad (3)$$

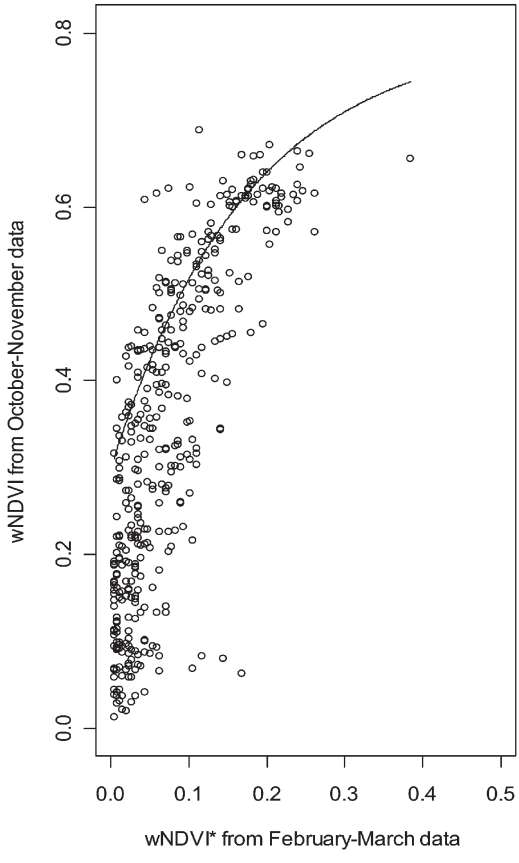

Figure 1. Winter NDVI based on observations during October and November described by Beck *et al*. (2006) versus winter NDVI based on observations during February and March (wNDVI*). The line shows the asymptotic exponential used to transform the winter NDVI based on observations during February and March (equation (2)).

We used the winter NDVI derived earlier as the minimum of the function and estimated the remaining five parameters using an iterative least-squares procedure.

2.4 *Estimating the parameters of the double logistic function*

The TIMESAT software package (Jönsson and Eklundh 2004, Jönsson and Eklundh 2006) was used to fit double logistic functions to time series for all pixels in the study area. TIMESAT uses a least-squares procedure to find the best fit by minimizing χ^2. The latter is the sum of squared differences between the NDVI values in the time series and the double logistic model function NDVI(t), which are weighted by w:

$$\chi^2 = \sum_{i=1}^{23} [w_i(\mathrm{NDVI}_i - \mathrm{NDVI}(t_i))]^2. \quad (4)$$

To take into account that most noise in NDVI data—even in data classified as reliable by the usefulness index—is negatively biased, the parameters of the model function were determined in two steps. In the first step, the parameters of the model

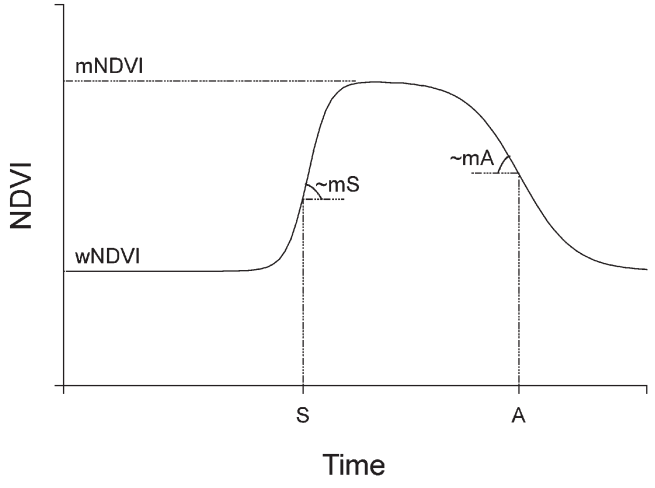

Figure 2. Example of the double logistic function NDVI(t) (equation (3)) used to model the yearly NDVI time series. It is defined by six parameters: the winter and maximum NDVI (wNDVI and mNDVI), two inflection points (S and A), and the rate of increase or decrease in NDVI at S and A, respectively (mS and mA).

function were obtained by minimizing χ^2 with weights w_i equal to 1. NDVI values below the model function of the first fit are thought of as less important, and in the second step the minimization was done with the weights w_i of the low data values decreased by a predefined factor. This two-step procedure leads to a model function that is adapted to the upper envelope of the data (figure 3).

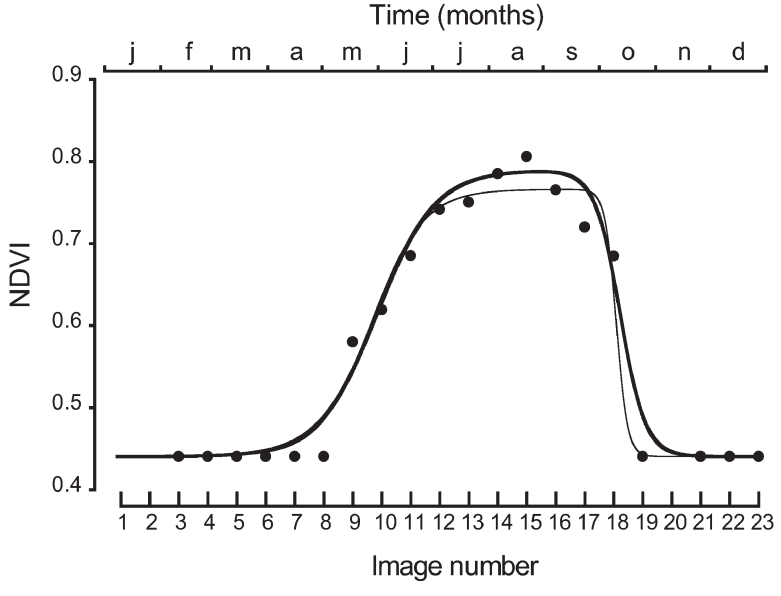

Figure 3. Two-step procedure for fitting the double logistic function to NDVI time series (shown as dots) after data filtering and correction. The result of the first step, an unweighted least-squares fitting procedure, is shown as a thin line. The result of the second step, a weighted least-squares fitting procedure, is shown as a thick line.

2.5 *Mapping spring and autumn phenology*

To map the start of the growing season, we estimated a threshold, termed 'spring NDVI', for each pixel *i*. The spring NDVI represents the NDVI value a pixel has when the vegetation in it enters the spring phenophase. In deciduous trees, this phenophase is the onset of leafing, and in coniferous trees it is the start of needle growth. We assumed that the spring NDVI was constant across years, and calculated it so that it represents 25% of the expected amplitude of the NDVI curve:

$$\text{springNDVI}_i = \text{wNDVI}_i + 0.25(\text{emNDVI}_i - \text{wNDVI}_i) \quad (5)$$

$$\text{autumnNDVI}_i = \text{wNDVI}_i + 0.75(\text{emNDVI}_i - \text{wNDVI}_i), \quad (6)$$

where emNDVI=expected maximum NDVI, and wNDVI=winter NDVI.

The expected maximum NDVI was calculated as the median of the maximum of the fitted double logistic function for a pixel in the different years. The onset of spring in a pixel in a given year was then set to the date when the double logistic NDVI curve in that year first exceeded the spring NDVI of the pixel. We followed a parallel procedure to model the end of autumn, setting it to the date when the NDVI curve dropped below the autumn NDVI, which represents 75% of the amplitude of the NDVI curve (equation (6)). The choice of the spring threshold of 25% of the NDVI amplitude follows earlier work in the region by Karlsen *et al*. (2001). They namely used a threshold of 33% but did not adjust for the presence of snow. The choice of the autumn threshold of 75% of the NDVI amplitude was based on a calibration using the data from the station at Kolari in Finland, which had the highest number of years with a recording of the autumn phenophase, namely five.

2.6 *Filtering the modelling output*

The modelled NDVI values were not considered reliable when the maximum difference between the modelled NDVI curve and the MVC data exceeded 30% of the range of the smoothed NDVI. For years and pixels where this was the case, estimates of phenology were not produced. Large differences indicate that the MVC time series showed large, inconsistent, and abrupt changes. These can be due to noise in the data or to the fact that the pixel does not cover natural vegetation. In addition, an estimate of the onset of spring was not produced for a pixel if more than one data point in the MODIS MVC data for the period between 22 March and 27 July was eliminated in the quality check. This is the period in which green-up occurs, and missing data can have a disproportionate influence on the results. Similarly, an estimate of the end of autumn was not produced if data were missing for the period between 29 August and 31 October.

2.7 *Validating the maps of the start of the growing season*

2.7.1 Ground observations of birch phenology. We compiled a validation dataset of ground observations of the onset of leafing and the end of leaf fall of downy and silver birch (*Betula pubescens* Ehrh. and *Betula pendula* Roth., respectively). Birch is the most common deciduous tree species in large parts of Fennoscandia (Bohn *et al*. 2000, Köble and Seufert 2001). Owing to its deciduous growth form, its phenophases are distinguished relatively easily. Here, the onset of leafing is defined as the date when leaves have emerged from more than 50% of leaf buds. The dataset

was compiled from our own observations, from data from Norwegian meteorological stations, and from various databases of observations gathered at research stations and by secondary school students (Schuck *et al*. 2002, GLOBE 2005, NML (Nettverk for miljølære) 2005). Assessing the accuracy of the dates, as well as the geographic coordinates in the last databases, was unfortunately difficult. We assumed that data were sufficiently reliable if the provided coordinates coincided with birch forest as indicated by land cover maps, and thus selected 64 data points. These were used together with 48 data points resulting from our own observations and meteorological stations (later referred to as quality-checked data points) for use in the validation (figure 4). The data points were unevenly distributed between years, with 17 observations in 2000, 15 in 2001, 20 in 2002, seven in 2003, 24 in 2004, and 29 in 2005.

Few ground data were available for validating the autumn phenophase: to be precise, seven observations in 2000, eight in 2001, five in 2002, three in 2003, three in 2004, and three in 2005 recorded the end of leaf fall in birch.

2.7.2 Validation procedure. We used two statistics to quantify the agreement between the ground observations and the modelled maps, namely the RMSE and the coefficient of determination (r^2). The coefficient of determination quantifies how much of the variance in the observed dates is explained by the model. The RMSE, on the other hand, is a measure of the average error of the predictions expressed in days.

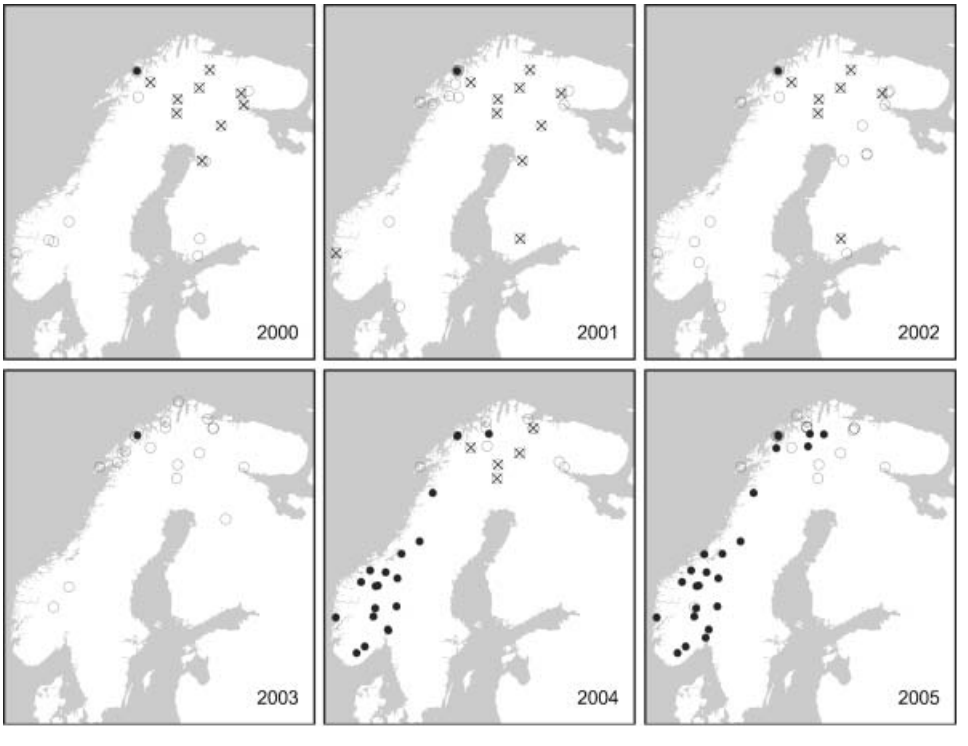

Figure 4. Registrations of birch phenology in Fennoscandia in the period 2000–2005. Solid dots show our own observations of bud burst and those gathered at Norwegian meteorological stations. Circles represent data points from other sources. Crosses indicate observations of the end of leaf fall.

Using linear regression models and Tukey's honestly significantly difference (HSD) procedure, we tested whether the agreement between the NDVI-derived dates and the ground observations differed along gradients of latitude and longitude and between years. The linear models had latitude, longitude, altitude or coniferous forest cover as the predictor variable, and prediction error (i.e. estimated date – observed date) as the response variable. The resulting least-squares parameter estimates (PE) and their standard errors (SE) quantified the dependency of the prediction error on the spatial gradients. T tests were included to assess the statistical significance of these dependencies. The HSD test was used to test whether the bias in the predictions differed between years. Finally, the precision of the predictions, quantified as |error-bias|, was compared between years, using Levene's test for homogeneity of variance (Levene 1960).

3. Results

3.1 *Winter NDVI map*

Replacing NDVI values during the winter season with the winter NDVI ensures that the rise in NDVI associated with the melting of snow is not mistaken for the green-up of vegetation in spring. This is particularly applicable in the case of coniferous forests, which are evergreen and are thus expected to display an NDVI higher than that of deciduous forests during winter. To test this, we compared the winter NDVI map with a map of coniferous forest cover that had a spatial resolution of 1 km and was derived from NOAA AVHRR data (Schuck *et al.* 2002) (figure 5). We compared the correlation between the coniferous cover and the winter NDVI at different scales. This was done by averaging the data in the maps, using windows ranging from 1×1 km to 14×14 km and using 600 points randomly located in the study area. The correlation between coniferous forest cover and winter NDVI increased as the window size increased, but only marginally when using windows larger than 5×5 km (figure 6).

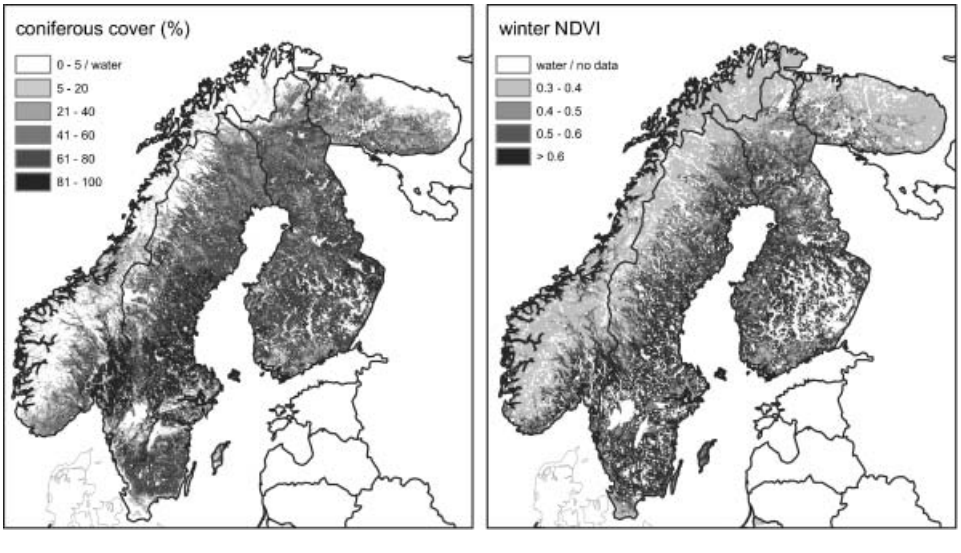

Figure 5. Winter NDVI and map of coniferous forest based on NOAA AVHRR data (Schwartz and Reed 1999).

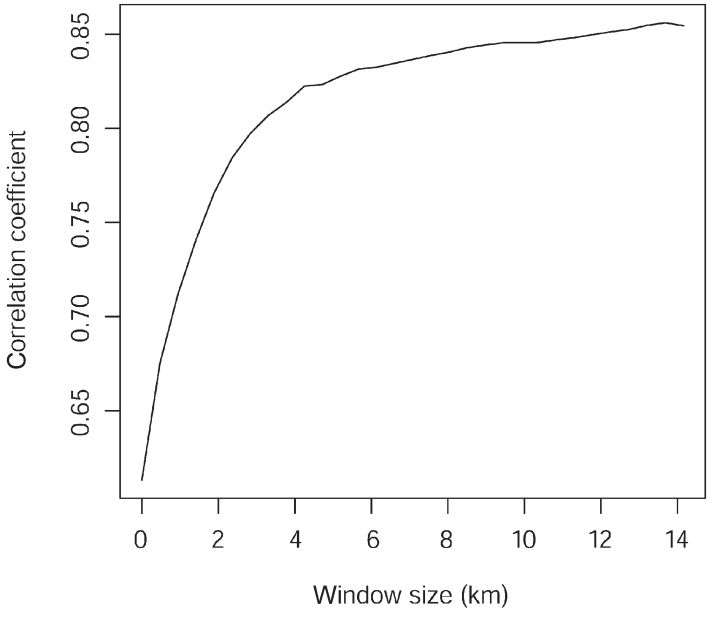

Figure 6. Correlation coefficients of winter NDVI and coniferous cover based on 600 points randomly located in the study area and after averaging square windows of pixels.

3.2 *Validation of phenological maps*

The predicted onset of the growing season correlates well with the observed onset of leafing of birch ($r^2=0.49$) and mimicked it with an RMSE of 12 days ($n=31$; figure 7(*a*)). This was assessed by extracting the predicted green-up date from each pixel coinciding with a phenological observation.

Green-up was not predicted for a number of pixels in the maps (§2.6). Consequently, not all ground data could be used in the validation procedure because there were no predicted dates for some pixels matching ground observations. To overcome this, we used data from a window of pixels covering the ground observation, rather than a single pixel. We tested the correlation between the means of 5 by 5 km windows and the ground observations. The correlation between the modelled and the observed dates was only slightly lower ($r^2=0.48$ vs 0.49) than that produced using the single-pixel approach, and the RMSE was similar (12 days). The advantage of this method was that it provided an estimate for almost all ground observations ($n=108$; figure 7(*b*)). Hence, we used the same 5×5 km averaging window both to produce phenological maps and for their further validation.

The phenological maps agreed better with the quality-checked data than with the observations retrieved from other databases, both when considering single pixels ($r^2=0.54$ vs 0.45) and when using the window averaging approach ($r^2=0.56$ vs 0.43).

While the errors did not vary with latitude, longitude, or coniferous forest cover ($PE_{lat}=-0.3$, $SE=0.3$, $p=0.3$, $PE_{lon}=-0.2$, $SE=0.1$, $p=0.1$, $PE_{conif}=-0.02$, $SE=0.04$, $p=0.6$), they did appear to increase with elevation by 1 day per 100 m of altitude ($SE_{alt}=0.5$ day per 100 m, $p=0.04$). The errors in the estimated onset of spring differed slightly between years, with the predicted dates ranging from 3 days

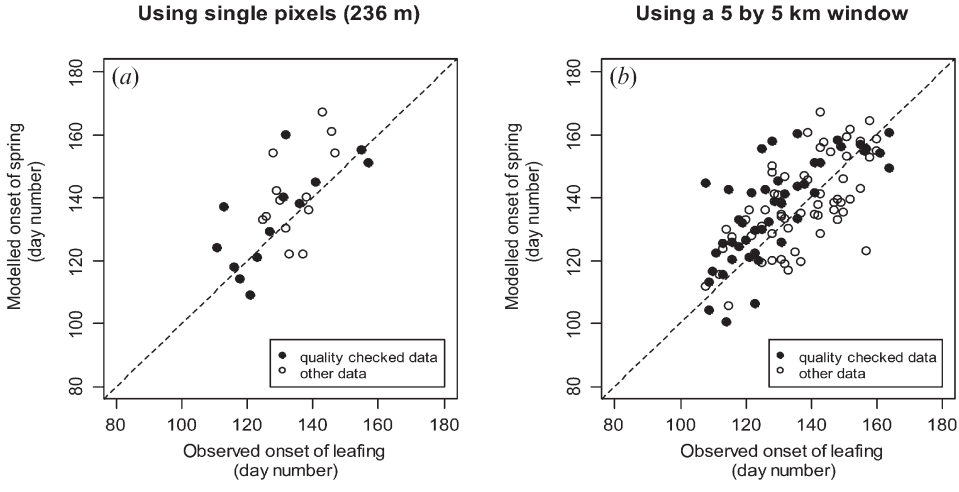

Figure 7. Scatter plots of the modelled onset of spring versus the *in situ* observed onset of leafing of birch, using (*a*) the pixel covering the site of the observation and (*b*) the mean of a window of pixels covering the site of the observation.

earlier on average than observed dates in 2003 (SE=5 days) to 6 days later in 2004 (SE=4 days). However, these differences in bias were not statistically significant (Tukey HSD test, $p > 0.1$ for all pairs of years), nor were the differences in precision, expressed as |prediction – bias|, between years (Levene's test, $F=0.41$, $p=0.52$).

The record of observations of autumn phenophases was sparse compared with that of observations of spring phenophases. This limited the degree to which the modelled maps of autumn could be validated. Here, we used the same approach as with the spring maps. First, we extracted data from the single pixels coinciding with ground observations. This produced only five data points (figure 8(*a*)) that coincided fairly well with the ground observations (RMSE=4.5 days, $r^2=0.8$). When using the 5×5 km windows to extract data from the maps, we obtained 26 data points. However, the correlation with the ground observations was poorer (RMSE=10 days, $r^2=0.27$) than with the single pixel approach, largely due to the presence of one outlier (without the outlier, RMSE=8 days, $r^2=0.44$; figure 8(*b*)).

The errors of the predictions did not change with latitude, longitude, altitude, or coniferous forest cover ($PE_{lat}=1.3$, SE=0.79, $p=0.1$, $PE_{lon}=0.32$, SE=0.39, $p=0.4$, $PE_{alt}=0.0046$, SE=0.020, $p=0.8$, $PE_{conif}=0.02$, SE=0.06, $p=0.8$). It should be noted, however, that the ground data concerning the autumn phenophase were predominantly recorded in the north of Fennoscandia. Consequently, the validation of the predictions of the end of autumn is less reliable for the south of Fennoscandia than for the north. Owing to the paucity of data available on autumn ground phenology, the difference in bias and precision between years could not be assessed.

3.3 *Onset of spring and end of autumn in Fennoscandia*

To map the mean onset of spring and end of autumn in the years 2000–2005 throughout the entire study area, we used the mean filter with a 5×5 km window. The spring maps show a distinct south–north gradient for the onset of spring, as well as an oceanic–continental gradient and an altitudinal gradient (figure 9). Within the

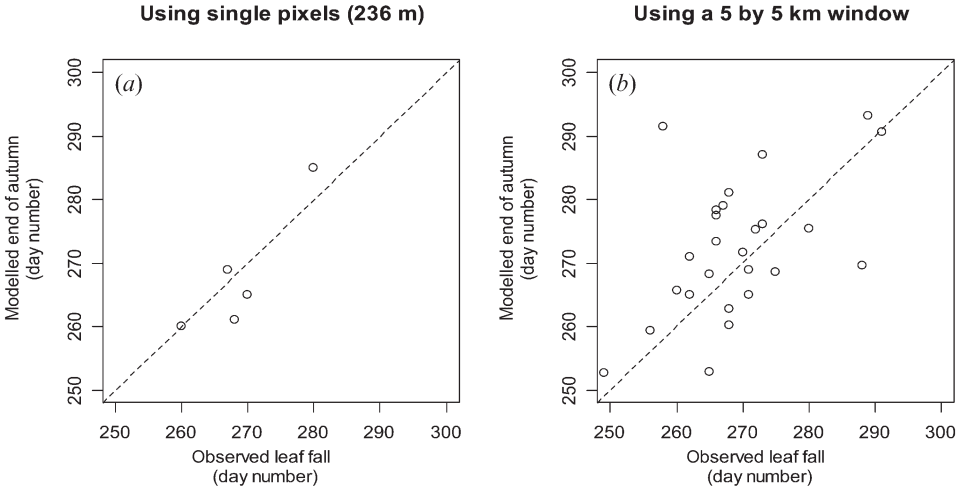

Figure 8. Scatter plots of the modelled end of autumn versus the *in situ* observed timing of leaf fall, using (*a*) the pixel covering the site of the observation and (*b*) the mean of a window of pixels covering the site of the observation.

study area, the onset of spring varies by more than two months: between the second week of April and the last week of June. Differences between years at the same location amount to as much as one month (figure 10). In comparison with the maps of spring, the maps of autumn correlate less with the altitudinal and south–north gradients. This could be an effect of the larger proportion of agricultural land in the south of the area. The maps indicate a range in the timing of the end of autumn of about one and a half months: from the second week of September to the last week of October (figure 9).

4. Discussion

The NDVI dataset presented here is created from MODIS 16-day MVC data and relies on the estimation of the winter NDVI, as well as a double logistic smoothing function. Here, however, both the influence of snow and the polar night and low-quality data have been removed, and missing values have been replaced. By describing the yearly NDVI trajectory of a pixel using the six parameters that define the double logistic function rather than 23 NDVI values, the size of the dataset has been reduced almost fourfold. This facilitates the use of the data for other applications.

The fact that the input data are 16 maximum value composites means that only one NDVI value is retained for every period of 16 days. However, the date of acquisition of the NDVI value selected to represent the 16-day period is not known, introducing a significant amount of uncertainty in the MVC dataset. Nevertheless, the validation of the dataset by mapping spring and autumn phenophases and comparing the results with ground data indicated good agreement in both cases. The ground data used for the validation described phenophases of downy and silver birch. While these are the dominant species in the study area, their abundance varied at the sites where observations were made. Hence, the NDVI trajectory observed over a pixel may have been significantly influenced by the greening of vegetation

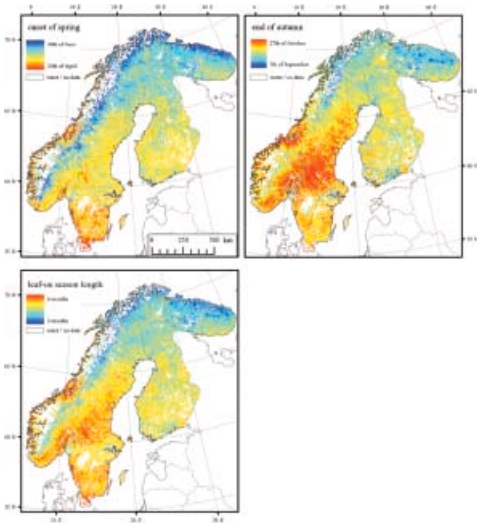

Figure 9. Mean onset of spring, mean end of autumn, and mean length of the period between budburst and leaf fall in Fennoscandia in the years 2000–2005. The maps were filtered using a mean filter with a window size of 5 × 5 km. Available in colour online.

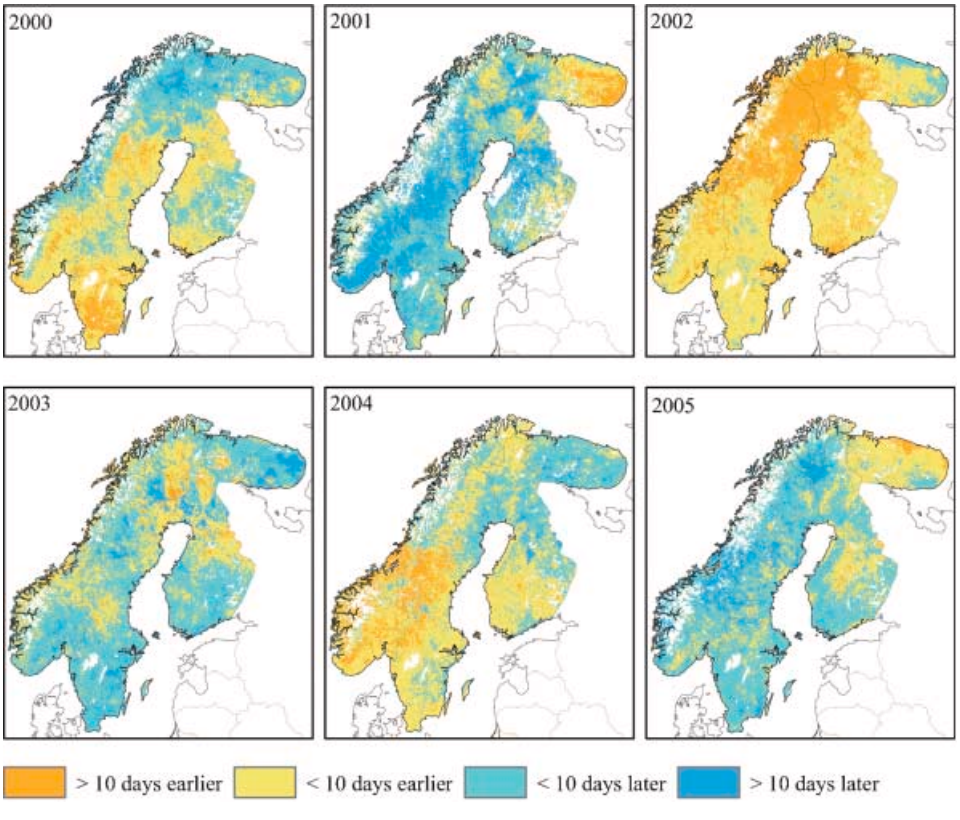

Figure 10. Anomalies in the onset of spring in the years 2000–2005, measured in relation to the mean onset of spring of the six years. The maps were filtered using a mean filter with window size of 5 km × 5 km. Available in colour online.

other than birch. This may have caused part of the deviation between the phenological estimates and the ground data. The map of the mean end of autumn shows, for example, an earlier onset of autumn in the far south of Sweden than further north. This could be related to the very high abundance of coniferous trees in the latter region. These are likely to display a longer period of elevated greenness than deciduous trees, which are more abundant farther south. Similarly, as trees become sparser with increasing altitude, the NDVI signal is more influenced by ground vegetation and less by the canopy. While a paucity of birch trees might account for part of the deviation between ground data and phenological estimates, it should have only a small effect on the possibility of estimating differences in phenology between years, which are expected to be similar for coexisting tree species. Indeed, our results show that interannual differences in the onset of spring as observed on the ground were largely accounted for in the maps.

It is only in recent years that phenological maps derived from NDVI time series have been validated using ground phenological data (Lechowicz and Koike 1995). One reason for this is that a coordinated effort is needed to acquire such *in situ* data across a large area. Another reason is that the sensors providing useful NDVI time series limited the spatial resolution of the phenological maps. Recently, Delbart *et al.* (2005) mapped spring phenology across northern Eurasia using Pathfinder AVHRR data, which has a compositing period of 10 days, and achieved an RMSE of 8 days ($n=81$). To determine the spring NDVI, they relied on a method that used SPOT-VGT data and a newer index, the Normalized Difference Water Index, which decreases with snowmelt and increases with the greening of vegetation. On its own, this latter method had an even better agreement with the *in situ* data, with an RMSE of 7 days ($n=21$). The results are difficult to compare, however, with those reported here, as the compositing period of both these datasets is 10 days, and in the SPOT-VGT dataset the exact date of acquisition of each NDVI value is known. The methods of mapping the phenophases rely on the choice of minimum winter NDVI and a threshold in the expected NDVI amplitude to derive a phenological date from the time series. These choices also impact the accuracy of the estimates, adding to the difficulty of comparing the adequacy of different methods.

In contrast to spring phenology, maps and ground data on autumn phenology are quite rare in the literature. Karlsen *et al.* (2006) mapped the start and end of the growing season in Fennoscandia using the AVHRR GIMMS dataset (GIMMS, 2005). At single stations, the correlation between observed and modelled spring dates varied greatly, between $r^2=0.04$ and $r^2=0.64$ for stations with six and nine observations, respectively. For autumn dates, observations were fewer, and correlation values varied even more, from $r^2=0.01$ to $r^2=0.97$ for stations with five and four observations, respectively. White *et al.* (1997) mapped the start and end of greenness in the continental United States using daily AVHRR NDVI data. They found a higher correlation with *in situ* data than that reported here, when considering not only the onset of greenness ($r^2=0.57$, $n=24$ vs $r^2=0.48$, $n=108$) but also the end of greenness, or in our case the end of leaf fall ($r^2=0.39$, $n=15$, vs $r^2=0.27$, $n=26$). When modelling the autumn phenophase, however, all studies had only a small body of validation data available. Nevertheless, the results reported here indicate that autumn phenology in Fennoscandia can be mapped using the modelled MODIS NDVI dataset. This is important, as the timing of the end of the growing season is crucial for modelling parameters such as the length of the growing season and annual productivity.

Locally and at their highest resolution, the maps can model the phenophases in different years well—although model output may be missing for a number of pixels. In all, this makes this the first dataset that enables vegetation phenology in Fennoscandia to be mapped at a spatial resolution as high as 250 m. But when producing maps at this resolution, it is crucial that the validation data are reliable and their geolocation accurate.

In conclusion, a smoothed NDVI dataset has been generated that enables phenology in Fennoscandia and the Kola peninsula to be mapped at a spatial resolution of 250 m. These data contain annual NDVI trajectories that will be useful for climatic and ecological studies, as well as for studying phenological variations in time and space across the region. Although the remotely sensed phenological maps correspond well with events observed on the ground, there is a need for additional validation data, especially for coniferous forests and the autumn phenophases.

Acknowledgements

We thank the students and teachers of the schools participating in 'Nettverk for miljølære' for gathering phenological data as well as Oddvar Jenssen for coordinating the phenological observations at the Norwegian Meteorological Institute. We are also grateful to the following persons for providing us with phenology data on birch: E. Kubin at the Finnish Forest Research Institute, Finland, Anna Tolvanen at the University of Oulu, S. Neuvonen at Kevo Subarctic Research Institute/University of Turku, Finland, P. S. Karlsson at Uppsala University, Sweden, PE Aspholm at Svanhovd Environmental Centre, Norway, Oddvar Skre, Norwegian Forest Research Institute Bergen, and to the archives of the Lapland Biosphere State Reserve, Kandalaksha Sate Nature Reserve, Pasvik Nature Reserve, and the Polar-Alpine Botanical Garden at Kirovsk. We would like to thank Nigel Yoccoz, for his advice on statistics, and two anonymous referees, for their comments on the manuscript. The information about the coniferous forest cover is based on the output from the project 'Forest tree groupings database of the EU-15 and pan-European area derived from NOAA-AVHRR data', which was awarded by the European Commission, Joint Research Centre (Institute for Environment and Sustainability), to a consortium consisting of EFI, VTT Information Technology and the University of Joensuu under the contract number: 17223-2000-12 F1SCISPFI. Funding for the work presented here was obtained from the Norwegian Research Council through the Phenoclim project.

References

Anyamba, A. and Tucker, C.J., 2005, Analysis of Sahelian vegetation dynamics using NOAA-AVHRR NDVI data from 1981–2003. *Journal of Arid Environments*, **63**, pp. 596–614.

Azzali, A. and Menenti, M., 2000, Mapping vegetation–soil complexes in southern Africa using temporal fourier analysis of NOAA AVHRR NDVI data. *International Journal of Remote Sensing*, **21**, pp. 973–996.

Badeck, F.-W., Bondeau, A., Böttcher, K., Doktor, D., Lucht, W., Schaber, J. and Sitch, S., 2004, Responses of spring phenology to climate change. *New Phytologist*, **162**, pp. 295–309.

Bailey, S.-A., Horner-Devine, M.C., Luck, G., Moore, L.A., Carney, K.M., Anderson, S., Betrus, C. and Fleishman, E., 2004, Primary productivity and

species richness: relationships among functional guilds, residency groups and vagility classes at multiple spatial scales. *Ecography*, **27**, pp. 207–217.

BARET, F. and GUYOT, G., 1991, Potentials and limits of vegetation indices for LAI and APAR assessment. *Remote Sensing of Environment*, **35**, pp. 161–173.

BECK, P.S.A., ATZBERGER, C., HØGDA, K.A., JOHANSEN, B. and SKIDMORE, A.K., 2006, Improved monitoring of vegetation dynamics at very high latitudes: a new method using MODIS NDVI. *Remote Sensing of Environment*, **100**, pp. 321–334.

BOHN, U., KATARINA, G.D. and WEBER, H., 2000, *Map of the Natural Vegetation of Europe. Scale 1 : 2 500 000* (Bonn: Federal Agency for Nature Conservation).

CHEN, J., JÖNSSON, P., TAMURA, M., GU, Z., MATSUSHITA, B. and EKLUNDH, L., 2004, A simple method for reconstructing a high-quality NDVI time-series data set based on the Savitzky-Golay filter. *Remote Sensing of Environment*, **91**, pp. 332–344.

DE BEURS, K.M. and HENEBRY, G.M., 2005, Land surface phenology and temperature variation in the IGBP High-Latitude transects. *Global Change Biology*, **11**, pp. 779–790, doi:710.1111/j.1265–2486.2005.00949.x.

DELBART, N., KERGOAT, L., LE TOAN, T., LHERMITTE, J. and PICARD, G., 2005, Determination of phenological dates in boreal regions using normalized difference water index. *Remote Sensing of Environment*, **97**, pp. 26–38.

DUCHEMIN, B., 1999, Potential and limits of NOAA-AVHRR temporal composite data for phenology and water stress monitoring of temperate forest ecosystems. *International Journal of Remote Sensing*, **20**, pp. 895–917.

GLOBE, 2005, The GLOBE Program. Available online at: http://www.globe.gov.

GIMMS (Global Inventory Monitoring and Modeling Studies), 2005, National Aeronautics and Space Administration. GIMMS NDVI. Available online at: http://ltpwww.gsfc.nasa.gov/gimms/htdocs/ndvi/ndvi/GIMMS.

GOETZ, S.J. and PRINCE, S.D., 1996, Remote sensing of net primary production in boreal forest stands. *Agricultural and Forest Meteorology*, **78**, pp. 149–179.

GONG, D.-Y. and SHI, P.-J., 2003, Northern hemispheric NDVI variations associated with large-scale climate indices in spring. *International Journal of Remote Sensing*, **24**, pp. 2559–2566.

GUYOT, G., GUGON, D. and RIOM, J., 1989, Factors affecting the spectral response of forest canopies: a review. *Geocarta International*, **3**, pp. 43–60.

HEUMANN, B.W., EKLUNDH, L., SEAQUIST, J.W. and JÖNSSON, P., 2007, Phenological change in the Sahel, Africa, 1982–2005. *Remote Sensing of Environment,* in press.

HOLBEN, B.N., 1986, Characteristics of maximum-value composite images for temporal AVHRR data. *International Journal of Remote Sensing*, **7**, pp. 1435–1445.

HUETE, A., DIDAN, K., MIURA, T., RODRIGUEZ, E.P., GAO, X. and FERREIRA, L.G., 2002, Overview of the radiometric and biophysical performance of the MODIS vegetation indices. *Remote Sensing of Environment*, **83**, pp. 195–213.

HØGDA, K.A., KARLSEN, S.R. and SOLHEIM, I., 2001, Climatic change impact on growing season in Fennoscandia studied by a time series of NOAA AVHRR NDVI data. In *IGARSS '01*, 9–13 July 2001, Sydney, pp. 1338–1340.

HØGDA, K.A., KARLSEN, S.R., SOLHEIM, I., TØMMERVIK, H. and RAMFJORD, H., 2002, The start dates of birch pollen seasons in Fennoscandia studied by NOAA AVHRR NDVI data. In *IGARSS '02*, 24–28 June 2002, Toronto, pp. 3299–3301.

HØGDA, K.A. and TØMMERVIK, H., 1998, Detection of caterpillar outbreaks in mountain birch forests. In *27th International Symposium on Remote Sensing of Environment*, 8–12 June 1998, Tromsø, Norway, pp. 532–534.

JÖNSSON, P. and EKLUNDH, L., 2002, Seasonality extraction by function fitting to time-series of satellite sensor data. *IEEE Transactions on Geoscience and Remote Sensing*, **40**, pp. 1824–1832.

JÖNSSON, P. and EKLUNDH, L., 2004, TIMESAT—a program for analyzing time-series of satellite sensor data. *Computers & Geosciences*, **30**, pp. 833–845.

JÖNSSON, P. and EKLUNDH, L., 2006, TIMESAT 2.2 available for download at http://www.natgeo.lu.se/personal/Lars.Eklundh/TIMESAT/timesat.html (accessed 15 July 2006).

JUSTICE, C.O., TOWNSHEND, J.R.G., HOLBEN, B.N. and TUCKER, C.J., 1985, Analysis of the phenology of global vegetation using meteorological satellite data. *International Journal of Remote Sensing*, **6**, pp. 1271–1318.

KARLSEN, S.R., ELVEBAKK, A., HØGDA, K.A. and JOHANSEN, B., 2006, Satellite based mapping of the growing season and bioclimatic zones in Fennoscandia. *Global Ecology and Biogeography*, **15**, pp. 416, DOI: 410.1111/j.1466–1822x.2006.00234.x.

KARLSEN, S.R., HØGDA, K.A., JOHANSEN, B., ELVEBAKK, A. and TØMMERVIK, H., 2001, Use of AVHRR NDVI data to map vegetation zones in north-western Europe (Poster presentation). In *29th International Symposium on Remote Sensing of Environment (ISRSE)*, 8–12 April 2002, Buenos Aires.

KÖBLE, R. and SEUFERT, G., 2001, Novel maps for forest tree species in Europe. In *8th European Symposium on the Physio-Chemical Behaviour of Air Pollutants: 'A Changing Atmosphere!'*, 17–20 September 2001, Turin, Italy.

LECHOWICZ, M.J. and KOIKE, T., 1995, Phenology and seasonality of woody plants: an unappreciated element in global change research? *Canadian Journal of Botany*, **73**, pp. 147–148.

LEVENE, H., 1960, Robust tests for equality of variances. Contributions to probability and statistics. In *Essays in Honor of Harold Hotelling*, I. Olkin, S.G. Ghurye, W. Hoeffding, W.G. Madow and H.B. Mann (Eds), pp. 278–292 (Stanford, CT: Stanford University Press).

LOS, S.O., JUSTICE, C.O. and TUCKER, C.J., 1994, A global 1 degree by 1 degree NDVI data set for climate studies derived from the GIMMS continental NDVI. *International Journal of Remote Sensing*, **15**, pp. 3493–3518.

LOS, S.O., NORTH, P.R.J., GREY, W.M.F. and BARNSLEY, M.J., 2005, A method to convert AVHRR Normalized Difference Vegetation Index time series to a standard viewing and illumination geometry. *Remote Sensing of Environment*, **99**, pp. 400–411.

MALINGREAU, J.P., 1986, Global vegetation dynamics: Satellite observations over Asia. *International Journal of Remote Sensing*, **7**, pp. 1121–1146.

MALINGREAU, J.P. and TUCKER, C.J., 1988, Large-scale deforestation in the southeastern Amazon basin of Brazil. *Ambio*, **17**, pp. 49–55.

MCCARTHY, J.J., CANZIANI, O.F., LEARY, N.A., DOKKEN, D.J. and WHITE, K.S., 2001, *Climate Change 2001: Impacts, Adaptation, and Vulnerability. Contribution of Working Group II to the Third Assessment Report of the Intergovernmental Panel on Climate Change* (Cambridge: Cambridge University Press).

MOEN, A., 1999, *National Atlas of Norway: Vegetation* (Hønefoss, Norway: Norwegian Mapping Authority).

NML (Nettverk for miljølære), 2005, Phenology of the North Calette. Bergen, Skolelaboratoriet i realfag, Universitetet i Bergen. Available online at: http://sustain.no/data/ut/activities/bn2a/.

OINDO, B.O. and SKIDMORE, A.K., 2002, Interannual variability of NDVI and species richness in Kenya. *International Journal of Remote Sensing*, **23**, pp. 285–298.

PETTORELLI, N., VIK, J.O., MYSTERUD, A., GAILLARD, J.-M., TUCKER, C.J. and STENSETH, N.C., 2005a, Using the satellite-derived NDVI to assess ecological responses to environmental change. *Trends in Ecology & Evolution*, **20**, pp. 503–510.

PETTORELLI, N., WELADJI, R.B., HOLAND, Ø., MYSTERUD, A., BREIE, H. and STENSETH, N.C., 2005b, The relative role of winter and spring conditions: linking climate and landscape-scale plant phenology to alpine reindeer body mass. *Biology Letters*, **1**, pp. 24–26.

PICARD, G., QUEGAN, S., DELBART, N., LOMAS, M.R., LE TOAN, T. and WOODWARD, F.I., 2005, Bud-burst modelling in Siberia and its impact on quantifying the

carbon budget. *Global Change Biology*, **11**, pp. 2164 doi:2110.1111/j.1365–2486.2005.01055.x.

SCHUCK, A., VAN BRUSSELEN, J., PÄIVINEN, R., HÄME, T., KENNEDY, P. and FOLVING, S., 2002, *Compilation of a Calibrated European Forest Map Derived from NOAA-AVHRR Data. EFI Internal Report 13* (Joensuu, Finland: European Forest Institute).

SCHWARTZ, M.D. and REED, B.C., 1999, Surface phenology and satellite sensor-derived onset of greenness: an initial comparison. *International Journal of Remote Sensing*, **20**, pp. 3451–3457.

SCHWARTZ, M.D., REED, B.C. and WHITE, M.A., 2002, Assessing satellite-derived start-of-season measures in the conterminous USA. *International Journal of Climatology*, **22**, pp. 1793–1805.

SELLERS, P.J., TUCKER, C.J., COLLATZ, G.J., LOS, S.O., JUSTICE, C.O., DAZLICH, D.A. and RANDALL, D.A., 1994, A global 1 by 1 NDVI data set for climate studies: 2. The generation of global fields of terrestrial biophysical parameters from the NDVI. *International Journal of Remote Sensing*, **151**, pp. 3519–3545.

STÖCKLI, R. and VIDALE, P.L., 2004, European plant phenology and climate as seen in a 20-year AVHRR land-surface parameter dataset. *International Journal of Remote Sensing*, **10**, pp. 3303–3330.

SUZUKI, R., NOKAMI, T. and YASUNARI, T., 2003, West-east contrast of phenology and climate in northern Asia revealed using a remotely sensed vegetation index. *International Journal of Biometeorology*, **47**, pp. 126–138.

TUHKANEN, S., 1980, Climatic parameters and indices in plant geography. *Acta Phytogeographica Suecica*, **67**, pp. 1–105.

VERMOTE, E.F., EL SALEOUS, N.Z. and JUSTICE, C.O., 2002, Atmospheric correction of MODIS data in the visible to middle infrared: first results. *Remote Sensing of Environment*, **83**, pp. 97–111.

WALKER, D.A., EPSTEIN, H.E., JIA, G.J., BALSER, A., COPASS, C., EDWARDS, E.J., GOULD, W.A., HOLLINGSWORTH, J., KNUDSON, J., MAIER, H.A., MOODY, A. and RAYNOLDS, M.K., 2003, Phytomass, LAI, and NDVI in northern Alaska: Relationships to summer warmth, soil pH, plant functional types, and extrapolation to the circumpolar Arctic. *Journal of Geophysical Research*, **108**, pp. doi: 10.1029/2001JD000986.

WANG, J., RICH, P.M. and PRICE, K.P., 2003, Temporal responses of NDVI to precipitation and temperature in the central Great Plains, USA. *International Journal of Remote Sensing*, **24**, pp. 2345–2364.

WHITE, M.A., NEMANI, R.R., THORNTON, P.E. and RUNNING, S.W., 2002, Satellite evidence of phenological differences between urbanized and rural areas of the Eastern United States deciduous broadleaf forest. *Ecosystems*, **5**, pp. 260–277.

WHITE, M.A., THORNTON, P.E. and RUNNING, S.W., 1997, A continental phenology model for monitoring vegetation responses to interannual climatic variability. *Global Biogeochemical Cycles*, **11**, pp. 217–234.

WYLIE, B.K., JOHNSON, D.A., LACA, E., SALIENDRA, N.Z., GILMANOV, T.G., REED, B.C., TIESZEN, L.L. and WORSTELL, B.B., 2003, Calibration of remotely sensed, coarse resolution NDVI to CO_2 fluxes in a sagebrush–steppe ecosystem. *Remote Sensing of Environment*, **85**, pp. 243–255.

ZHANG, J., DONG, W., FU,, , C. and WU, L., 2003a, The influence of vegetation cover on summer precipitation in China: a statistical analysis of NDVI and climate data. *Advances in Atmospheric Sciences*, **20**, pp. 1002–1006.

ZHANG, J.Y., DONG, W.J., YE, D.Z. and FU, C.B., 2003b, New evidence for effects of land cover in China on summer climate. *Chinese Science Bulletin*, **48**, pp. 401–405.

ZHOU, L., KAUFMANN, R.K., TIAN, Y., MYNENI, R.B. and TUCKER, C.J., 2003, Relation between interannual variations in satellite measures of northern forest greenness and climate between 1982 and 1999. *Journal of Geophysical Research*, **108**, pp. doi: 10.1029/2002JD002510.

ZHOU, L., TUCKER, C.J., KAUFMANN, R.K., SLAYBACK, D., SHABANOV, N.V. and MYNENI, R.B., 2001, Variations in northern vegetation activity inferred from satellite data of vegetation index during 1981 to 1999. *Journal of Geophysical Research*, **106**, pp. 20069–20083.